Impact-induced sublimation drives volatile depletion in carbonaceous meteorites

Zheng-Yu Long, Frederic Moynier, Tim F J Bögels, Linru Fang, Razvan Caracas, Marine Paquet, Fred Jourdan, Tu-Han Luu, Dimitri Rigoussen, Kun-Feng Qiu, et al.

nature communications

Article

https://doi.org/10.1038/s41467-025-61115-3

Impact-induced sublimation drives volatile depletion in carbonaceous meteorites

Received: 17 April 2025

Accepted: 13 June 2025

Published online: 03 July 2025

Check for updates

Zheng-Yu Long[1,2] ✉, Frederic Moynier[1] ✉, Tim F. J. Bögels[1], Linru Fang[1,3], Razvan Caracas[1,4,5], Marine Paquet[6], Fred Jourdan[7], Tu-Han Luu[1], Dimitri Rigoussen[1], Kun-Feng Qiu[2], Jun Deng[2] & James M. D. Day[8]

Carbonaceous chondrites are amongst the most chemically primitive solid materials in the Solar System, yet many are depleted in moderately volatile elements. Here, we report enrichments in heavier zinc isotopes in heated carbonaceous chondrites compared to the typical ranges for chondritic meteorites. Our results indicate that impact-driven thermal metamorphism under low-pressure conditions led to partial sublimation of zinc. First-principles calculations support that zinc escapes from solids in the absence of melting, consistent with shock heating and rapid outgassing. The resulting solid residue is strongly enriched in heavier Zn isotopes with minimal recondensation. These findings link extreme isotopic signatures to collisional processing, revealing that asteroid-scale impacts can drive volatile loss from undifferentiated asteroids. These carbonaceous chondrites provide the first unequivocal evidence for purely kinetic Zn isotope fractionation during volatilization. Impact-induced volatilization drives volatile depletion in asteroidal parent bodies, with implications for the delivery and distribution of volatiles in early planetary systems.

Chondrites, which are primitive meteorites formed 2–3 million years after the Solar System's formation[1], are considered foundational building blocks for terrestrial planets[2]. The evolution of moderately volatile elements (MVE) in chondrites provides key insights into the origin and depletion of volatiles on terrestrial planets. Unlike terrestrial planets, which have undergone extensive melting and differentiation, chondrites retain their original composition with two primary constituents, i.e., chondrules and matrix[1]. Chondrules are silicate-rich spherules formed by transient heating events in the protoplanetary disk, embedded within a fine-grained matrix that accreted at lower temperatures, preserving presolar grains and volatile compounds[3,4]. Among carbonaceous chondrites (CC), except for the Ivuna-type (CI) chondrites and samples returned from Ryugu and Bennu, which closely mirror the solar photosphere in their non-volatile element composition, there is a noticeable variation in the depletion of MVE correlated with their condensation temperatures[5–9].

An early protoplanetary disk is characterized by high temperatures (ranging from ~1000 to >2000 K) that could lead to dust vaporization and subsequent condensation, along with chondrule-forming events and giant impacts followed by magma oceans[4,10]. These processes likely facilitated the mobilization of MVE, including Zn. This is evidenced by the mass-dependent Zn isotopic fractionation (reported as δ^{66}Zn relative to JMC-Lyon) observed between chondrite groups[11]. Previous studies have identified a negative correlation between δ^{66}Zn and 1/[Zn] among different groups of carbonaceous chondrite[12–14], opposite to the expected trend if evaporation controls

[1]Université Paris Cité, Institut de Physique du Globe de Paris, CNRS, Paris, France. [2]State Key Laboratory of Geological Processes and Mineral Resources, Frontiers Science Center for Deep-time Digital Earth, School of Earth Sciences and Resources, China University of Geosciences, Beijing, China. [3]Centre for Star and Planet Formation, Globe Institute, University of Copenhagen, Copenhagen K, Denmark. [4]Center for Planetary Habitability (PHAB), University of Oslo, Oslo, Norway. [5]Research Institute of the University of Bucharest, University of Bucharest, Bucharest, Romania. [6]Université de Lorraine, CNRS, CRPG, Nancy, France. [7]Western Australian Argon Isotope Facility, John de Laeter Centre, School of Earth and Planetary Sciences, Curtin University, Perth, WA, Australia. [8]Scripps Institution of Oceanography, University of California San Diego, La Jolla, CA, USA. ✉e-mail: long@ipgp.fr; moynier@ipgp.fr

Zn abundance and isotopic fractionation. This has been interpreted as reflecting the mixing between an isotopically light/volatile poor- and an isotopically heavy/volatile rich- reservoir. Similarly, magmatic iron meteorites, representing the cores of early-formed asteroids, display this same relationship[15]. The origin of the light Zn isotopic composition of chondrules was suggested to reflect the removal of isotopically heavy Zn from chondrules (or their precursors) via sulfide segregation[13,16,17] or as a result of partial condensation processes[18], where Zn-depleted chondrites exhibited enrichment in lighter Zn isotopes. Again, evaporation most likely played a limited role in the volatile depletion observed in CC parent bodies or their precursors.

Despite these lines of evidence, several CC meteorites are highly depleted in volatile elements and display a trend of increasing δ^{66}Zn values coupled with decreasing Zn content[19]. These CC meteorites experienced heating processes by thermal metamorphism after the accretion of their parent body[20–22]. During these processes, light Zn isotopes might be volatilized, leaving the residual solid phase enriched in heavy Zn isotopes[19]. Heavy Zn isotope enrichments related to evaporation have been observed in lunar mare basalts, martian meteorites, impact melt sheets, impact glasses and tektites, and nuclear detonation materials[23–34]. Previous studies indicate that, compared to theoretical predictions, actual evaporation is likely to generate a subdued isotopic fractionation[35]. A limited fractionation model for Zn isotopes was further proposed to explain various planetary evaporation events under impact-related conditions[34]. However, extremely high δ^{66}Zn values reported in heated CC chondrites (up to 16.7‰; Fig. 1)[19] exceed those predicted by these models.

To address this discrepancy and further explore the behavior of Zn during volatilization from a solid state, we analyzed the Zn isotopic compositions of eight heated CC meteorites from Antarctica, including heated CM chondrites and CY (Yamato-type) chondrites. These meteorites record extensive aqueous and thermal alteration, followed by relatively short-lived thermal metamorphism[19,22,36]. CY chondrites, a recently recognized group of CCs, are considered to potentially be thermally metamorphosed CI chondrites[36–39], as documented to exhibit notably heavy O isotopic compositions similar to the CI field (Fig. S1). We also estimate the relative evaporation of Zn, Cd, Fe, and Mg from solid materials from first-principles calculations. Altogether, we demonstrate that evaporative loss by impacts significantly contributes to the volatile depletion in chondritic parent bodies.

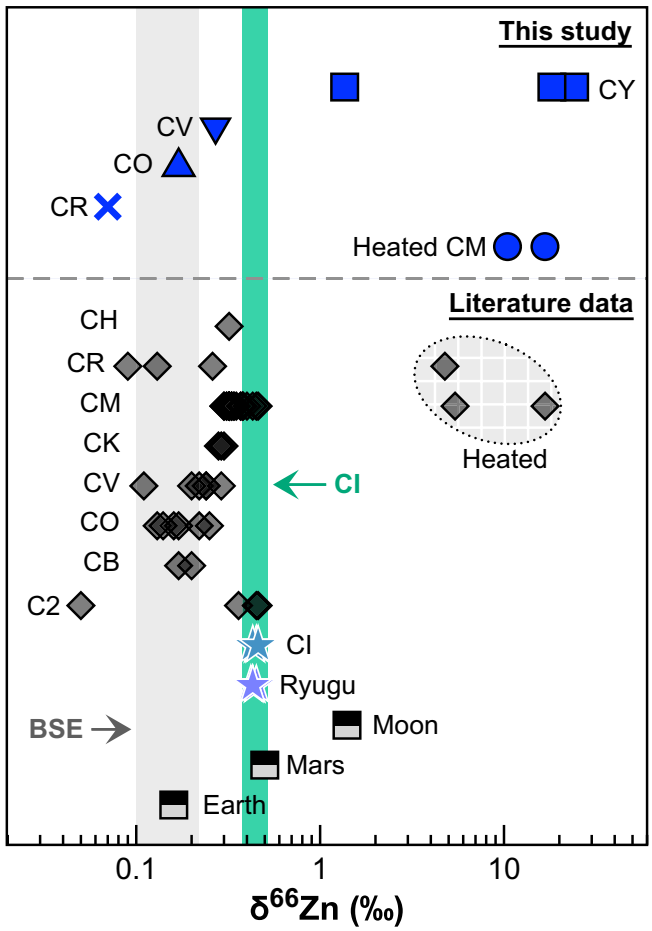

Fig. 1 | Zinc isotopic compositions of the investigated carbonaceous chondrites. Also shown are the reported materials in the literature[12–14,19,25,26,33,49,69,70]. The green shadow area represents the CI range (0.46 ± 0.08‰)[12,14,49]. The gray shadow area represents the BSE range (0.16 ± 0.06‰)[70].

Results and discussion

Samples

We analyzed a set of heated carbonaceous chondrites, including heated CM [Pecora Escarpment (PCA) 02010 and PCA 02012], CY [Yamato (Y)−86789, Y-86720, Belgica (B)−7904, among which Y-86789 is paired with Y-86720], CV [Asuka (A)−881655], CR (Y-793495) and CO (Y-790992) meteorites[36,40,41], to provide a diverse contextual framework. Our study primarily focuses on CM and CY samples, which display evidence of heating events, as indicated by their depleted volatile element abundances and water contents[19,21,41–43]. Two heated CM meteorites, PCA 02010 and PCA 02012, previously analyzed for their Zn isotopic compositions[19], were reassessed using different sample fractions. The two meteorites underwent significant heating at temperatures >900 °C[22,44], as indicated by their extremely heavy isotopic compositions of Zn, K, and Rb, resulting from evaporation from post-accretionary heating events[19,45,46]. The CM and CY samples were subjected to much shorter heating durations (ranging from hours to several years) compared to the prolonged thermal processing of CO and CV chondrites, which lasted millions of years[47]. The estimated temperature order of the other heated chondrites, based on open system heating severity, is 500 °C < A881655 < B-7904 < Y-86720 = Y-86789 (≥700 °C), with Y-86720 and Y-86789 specifically exhibiting thermal metamorphism above 700 °C[21,48]. Notably, B-7904 and, to a lesser extent, Y-86789 and Y-86720 differ from other CYs by clearly preserving chondrules or chondrule pseudomorphs[39,47]. Metamorphism has modified their mineralogy, with phyllosilicates recrystallizing into olivine and pyroxene[47].

Zinc contents and isotopic compositions

In this study, the analyzed carbonaceous chondrites show a wide range of Zn concentrations from 1.77 to 162 μg/g, with δ^{66}Zn values ranging from 0.07 to 24.2‰ (Fig. 1; Table S1). The CY chondrite samples exhibit lower Zn concentrations (31.0–162 μg/g) and higher δ^{66}Zn values (1.36–24.2‰) compared to the CI chondrites, which have relatively high Zn contents of 309 ± 44 μg/g and homogeneous δ^{66}Zn values of 0.46 ± 0.08‰[12–14,49]. Among the CYs, the paired CY samples display extremely high δ^{66}Zn values (18.2 ± 0.04‰ and 24.2 ± 0.01‰), which represent the highest δ^{66}Zn ever measured across all meteorites, including EL chondrites (a subgroup of enstatite chondrites known for heavy Zn isotope signatures)[50]. By comparison, B-7904, which is relatively rich in chondrules[47], displays a markedly lower δ^{66}Zn value, closer to the CI chondrite range. The heated CV, CR, and CO samples have δ^{66}Zn of 0.27 ± 0.01‰, 0.07 ± 0.02‰, and 0.17 ± 0.02‰, respectively, aligning within the typical ranges previously reported for these groups (Fig. 2). The two heated CM chondrites display significant depletion in Zn contents (1.77–14.9 μg/g) and enrichment in heavy Zn isotopes (δ^{66}Zn = 10.5–16.7‰). Two separate fragments of the CM chondrite PCA 02010 show slight differences in Zn contents (1.77 μg/g and 2.79 μg/g) and δ^{66}Zn (10.5 ± 0.09‰ and 11.3 ± 0.01‰). The δ^{66}Zn

https://doi.org/10.1038/s41467-025-61115-3

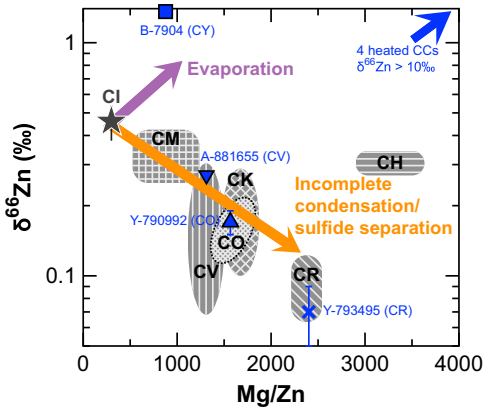

Fig. 2 | A plot of δ^{66}Zn against the Mg/Zn ratio. The ranges for various sub-groups of carbonaceous chondrites are after reference[13,14]. The colored arrows indicate the anticipated trends: one showing an increase in δ^{66}Zn values due to evaporation, and the other showing a decrease in δ^{66}Zn values resulting from incomplete condensation or sulfide separation.

values measured in this study also diverge from the previously reported value of 5.42‰ for PCA 02010[19]. This suggests isotopic heterogeneity within the individual PCA 02010 chondrite aliquots. Sample PCA 02012 exhibits a Zn content of 14.9 μg/g and δ^{66}Zn of 16.7‰, aligning with the earlier study[19].

Origin of elevated δ^{66}Zn in carbonaceous chondrites

This study demonstrates that the analyzed carbonaceous chondrites display a wide range of δ^{66}Zn values, extending beyond the typical range previously reported for these meteorites (Fig. 1). The CO, CV, and CR samples analyzed here exhibit δ^{66}Zn values consistent with those of their respective chondrite groups. In contrast, the paired CY (Y-86720 and Y-86789) and heated CM chondrites show exceptionally high δ^{66}Zn values relative to both CI chondrites and the typical carbonaceous chondrite range. Notably, the chondrule-rich CY sample B-7904 exhibits a significantly lower δ^{66}Zn value than other CYs, although it remains elevated relative to the broader carbonaceous chondrite trend (Fig. 1). Terrestrial contamination could influence isotopic compositions, however, no terrestrial samples, including continental crustal rocks (~0.28 ± 0.05‰)[51], reach the elevated levels observed in the measured samples. Additionally, the chondritic Sr/Mg and Ba/Mg ratios and REE patterns of the samples, which contrast with the typical light-REE enrichment and negative Eu anomaly of the upper continental crust (Fig. S4), further exclude terrestrial contamination as a contributing factor.

Although some carbonaceous chondrites (e.g., PCA samples) exhibit evidence of terrestrial weathering[21,52,53], terrestrial chemical weathering and alteration fail to account for the observed high δ^{66}Zn, given the resistance of Zn isotopes to aqueous alterations. For instance, weathered igneous rocks display δ^{66}Zn slightly lower or comparable to their unaltered igneous protoliths[54,55]. Furthermore, there is no correlation between fluid-mobile element concentrations (Pb/Th and Rb/Th) and δ^{66}Zn (Fig. S3). Aqueous alteration may also have preceded thermal metamorphism in the precursors of many CC chondrites[20,21]. However, aqueous alteration does not exert a first-order effect on volatile element concentrations[56]. In addition, no significant enrichment of heavy Zn isotopes was observed in those previously reported CC chondrites with aqueous alteration imprints[19], as well as the CR (Y-793495) and CO chondrites (Y-790992) in this study. The high δ^{66}Zn values are intrinsic signatures of these meteorites.

Fractionation of stable isotopes in multi-isotope space (e.g., δ^{68}Zn–δ^{66}Zn) follows different mass-dependent laws that can be used to distinguish between kinetic and equilibrium fractionation mechanisms[57,58]. Equilibrium fractionation typically occurs when different substances reach thermodynamic equilibrium, whereas kinetic fractionation takes place under nonequilibrium, unidirectional processes (such as rapid evaporation or diffusion). In three-isotope plots, the slopes or curves corresponding to kinetic and equilibrium processes marginally differ. For Zn isotopes, theoretical calculations predict the equilibrium fractionation slope in δ^{68}Zn–δ^{66}Zn space to be ~1.942, compared to 1.971 for kinetic fractionation of vapor-phase Zn. Furthermore, for ZnS and $ZnCl_2$ (common species involved in Zn loss during vaporization), the calculated kinetic fractionation slopes are 1.981 and 1.986, respectively, while the equilibrium fractionation slopes are 1.961 and 1.972. Detailed calculation methodologies are provided in the Supplementary Materials. The measured δ^{68}Zn–δ^{66}Zn mass-dependent slope for our samples is 1.985 ± 0.003 (Fig. S2), consistent, within analytical error, with theoretical predictions for kinetic evaporation. These CC chondrites offer the first evidence of purely kinetic Zn isotope fractionation occurring during volatilization.

Zinc isotopic fractionation mechanisms of carbonaceous chondrites

The increase in Mg/Zn ratios, coupled with decreasing δ^{66}Zn has been observed across different groups of carbonaceous chondrites[12,13]. The results from samples analyzed in this study also follow this pattern (Fig. 2). The compositional gradient from CI-like to CR chondrites, the latter marking the endpoint of volatile depletion, is indicative of the accretionary history involving the mixing of chemically and isotopically distinct reservoirs[12,18,37,46,59]. The correlation of δ^{66}Zn with stable Cr isotope anomalies ε^{54}Cr[13] supports the idea of mixing between isotopically heavy/volatile-rich matrix material and isotopically light/volatile-poor chondrule material, where either partial condensation following near-complete evaporation of Zn[50,60] or sulfide segregation during chondrule formation[13] leads to a predominance of light Zn isotopes in chondrules.

By contrast, in heated CM and CY samples, δ^{66}Zn values are elevated and Zn depletion is pronounced. This indicates that evaporation processes control Zn isotopic fractionations. Under high ambient pressures or in effectively closed systems, Zn evaporation yields only minimal isotopic fractionation[30,35,61]. The presence of a confining gas allows vapor to recondense onto solids (a back-reaction)[61,62], and limited Zn diffusion within the condensed phase further suppresses isotopic shifts[23,63]. As a result, in near-equilibrium evaporation at high temperatures, the fractionation factor (α) is approximately 1[63]. Experiments and natural analogs support this trend. In a 1-bar furnace, an experimental study observed α = ~0.996 in the air (rising to ~0.9978 under more reducing conditions)[63], whereas silicate melt glass from the Trinity nuclear test (formed at ~1 atm) recorded α = ~0.999–0.9995[28,30]. Similar high fractionation factors (mostly ranging from 0.999 to 0.9999)[34] are also inferred for lunar mare basalts, diogenites, tektites, and terrestrial impact glasses[23–27,29,30,60,64] (Fig. 3). Such high fractionation factors are inconsistent with rapid unidirectional evaporation and instead indicate near-equilibrium or diffusion-limited volatilization conditions.

In contrast, under low-pressure or vacuum conditions, evaporation follows a kinetic regime that strongly fractionates Zn isotopes[65]. With negligible recondensation, lighter isotopes escape preferentially, and the fractionation factor is controlled by mass differences of the evaporating species. Theoretical α values in free evaporation are far below unity: on the order of 0.9753 for atomic Zn vapor, 0.9897 for ZnS, and 0.9927 for $ZnCl_2$ (by taking the square root of the ratio of the mass numbers of the light and heavy isotopologues of the vaporizing species). This yields extremely heavy residual Zn isotope compositions (high δ^{66}Zn) in the remaining solids, as observed in the most volatile-depleted meteorites[19]. Indeed, heated carbonaceous chondrites that lost large fractions of Zn and other volatiles are highly enriched in heavy Zn isotopes, indicating an open-system evaporation process.

https://doi.org/10.1038/s41467-025-61115-3

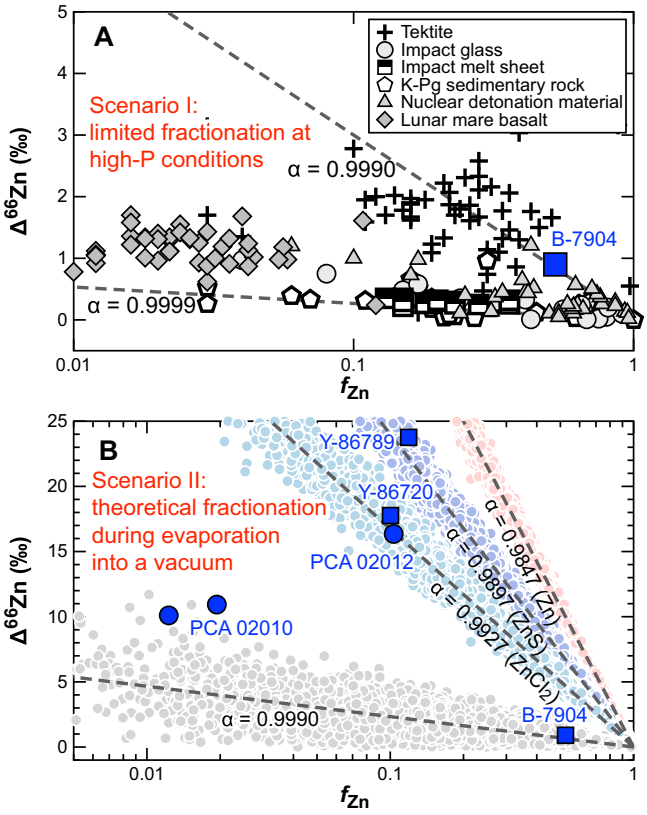

Fig. 3 | Plots showing Zn isotopic variation ($\Delta^{66}Zn = \delta^{66}Zn_{sample} - \delta^{66}Zn_{initial}$) versus the fraction of retained Zn (f_{Zn}) related to the Zn evaporative loss. Dashed lines represent the Zn isotopic fractionation factors. In (**A**), the α values range from 0.9999 to 0.9990, indicating the limited Zn isotopic fractionation expected under high-P conditions associated with impact events. The data sources of reported materials are summarized in reference[34]. In (**B**), theoretical fractionation factors for evaporation into a high vacuum are displayed (0.9753 for elemental Zn, 0.9897 for ZnS, and 0.9927 for $ZnCl_2$). The CI chondrites ([Zn] = 309 μg/g; $\delta^{66}Zn = 0.46‰$)[12,14,49] are used to represent the starting material for CY chondrites. The initial material for CM chondrites is based on the water- and volatile-rich CM sample Lonewolf Nunataks 94101 (LON 94101; [Zn] = 144 μg/g; $\delta^{66}Zn = 0.32‰$)[19]. Small colored dots in the background represent results from a Monte Carlo simulation. The simulation follows the Rayleigh distillation model: $\delta^{66}Zn = (1000 + \delta^{66}Zn_0) \times f^{\alpha-1} - 1000$, where $\delta^{66}Zn_0$ is the initial Zn isotopic composition, α is the fractionation factor, and f is the evaporative loss ratio of Zn. The $\delta^{66}Zn_0$ is assigned randomly following a normal distribution (mean ± σ_{SD}). The simulation incorporates isotopic fractionation under different scenarios characterized by α values of 0.9847 (±0.00005), 0.9897 (±0.00005), 0.9927 (±0.00005), and 0.9990 (±0.00005). Each scenario is simulated over 10,000 trials to ensure robust statistical outcomes. The f is randomly selected between 0 and 1 in each trial.

Using Monte Carlo simulations (modeling details in the caption of Fig. 3), we reproduce the elevated $\delta^{66}Zn$ in B-7904 (and to a lesser extent in PCA 02010) with an evaporation fractionation factor of $\alpha = 0.9990 \pm 0.00005$ (SD) (Fig. 3), consistent with an impact-induced volatilization under elevated pressure (although still in the kinetic regime). Under a more plausible limited-fractionation scenario, the isotopic heterogeneity observed among individual PCA 02010 chondrite aliquots may be governed by back-reactions and limited Zn diffusion within the condensed phase. Notably, other thermally metamorphosed chondrites (e.g., PCA 02012, Y-86789, and Y-86720) plot along expected Rayleigh fractionation trajectories, reinforcing that open-system kinetic evaporation with minimal back-reaction governed their Zn loss. Therefore, the collective evidence points to extensive Zn evaporation at high temperatures and relatively low ambient pressure, with only limited recondensation. Such conditions would produce pronounced kinetic isotope effects and leave the residual solids substantially enriched in heavy Zn isotopes.

Evaporation of zinc from the solid phase

Kinetic Zn isotope fractionation during volatilization observed here is distinctly different from the more subdued or mixed processes involving partial recondensation or melt-phase interactions. By contrast, the exceptionally high $\delta^{66}Zn$ values, along with the linear mass-dependent trend, demonstrate predominantly open-system kinetic evaporation. Thermal events responsible for heating CM chondrites occurred hundreds of millions (possibly even billions) of years after the formation of the Solar System, with a recent study suggesting an age of at least 3 Ga[22]. This timing rules out short-lived radionuclides as the heat source and instead points to collisions, which aligns with the collision ages associated with asteroid families[22]. Similarly, recent work suggests the CI parent body may have undergone collisional heating, producing partially dehydrated, "CY-like" materials that were then ejected[38]. A single impact could explain both the chemical similarities in non-volatile elements between CY and CI and their differences in water content and volatile inventories. Notably, these heated chondrites show no evidence of large-scale melting. Their mineral structures are consistent with solid-state metamorphism[21,48]. This raises the likelihood that Zn can be lost via evaporation from the solid state during impact heating and without extensive melting.

In this study, we performed first-principles calculations to evaluate the feasibility of Zn evaporation from a solid phase (Mg_2SiO_4) under vacuum and compared Zn loss with that of Cd, Mg, and Fe (Fig. 4). Our results indicate that both Zn and Cd can readily escape from the solid phase without melting, requiring less energy—and thus having a higher likelihood—to vaporize compared to Fe and Mg. Among these elements, Cd is lost most efficiently, followed by Zn, then Fe and Mg. An earlier study reported substantial Zn loss from CM2 chondrite (Murchison) under low-pressure (~10 Pa) heating between 400 and 1000 °C, most notably around 700 °C[66]. Taken together, these observations support that Zn can undergo significant vaporization from solid phases in the absence of melting. These findings also align well with observations in chondrites, where Cd generally exhibits stronger depletion relative to Zn, and Zn shows more pronounced depletion than less volatile elements[41,66]. In fact, carbonaceous chondrites are highly porous and volatile-rich. Compared with ordinary chondrites, they can reach higher post-shock temperatures under moderate shock pressures, and their threshold for partial melting is lower[67]. For instance, under shock pressures of ~20–30 GPa, local materials may be momentarily heated to ~600–800 °C[52], which is still below the melting threshold, consistent with the observation that not all heated CM chondrites show melting features. The vapor pressure of Zn is relatively high under low-pressure regimes[21,41,66]. Once temperatures exceed ~600 °C in near-vacuum conditions (as on the surface of an asteroid), Zn becomes prone to sublimation.

Although the high temperatures generated by impact shocks may last only milliseconds to seconds, this interval can still suffice for Zn volatilization. The evaporation rate at these temperatures is rapid, and shock-induced fracturing accelerates outgassing. Moreover, sulfide (strong affinity of Zn for sulfide phases such as troilite and sphalerite) decomposition above ~500 °C liberates sulfur gases that carry Zn and form Zn oxide or metal vapor (Fig. 3). Zinc does not require complete lattice-scale diffusion to be lost; instead, thermal decomposition and the creation of fracture surfaces can directly transfer Zn into pore spaces or thin melt layers, where it then evaporates. In an open system (e.g., near the surface where ejecta are dispersed), newly formed Zn vapor readily diffuses into space[68]. Consequently, recondensation of light Zn isotopes back into the rock is minimal, leading to an enrichment of heavy Zn isotopes in the residue. In our samples, pronounced heavy Zn isotopic compositions indicate that Zn vapor did not fully

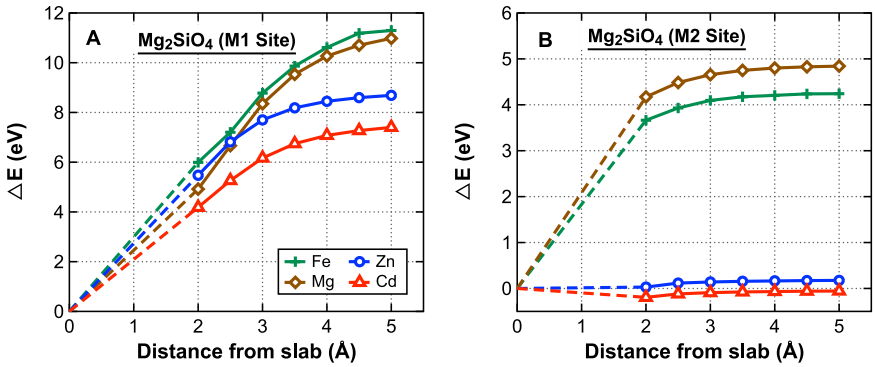

Fig. 4 | First-principles calculation results of evaporation energy (ΔE) versus distance from the slab. Energy difference as a function of distance to the surface for several divalent cations evaporating from the two, M1 (**A**) and M2 (**B**), sites of a slab of olivine placed in a vacuum, as obtained from first-principles calculations (details in Supplementary Materials). The plateau at high distances represents the complete evaporation state. The first 2 Å of displacement in each simulation is omitted because the energy differences in that region primarily reflect surface rearrangement structures rather than actual dissociation energies. The calculations show that Cd and Zn have lower ΔE values than Mg and Fe, indicating that Cd and Zn are more readily lost from the solid during evaporation. At the M2 site, Δ*E* for both Cd and Zn is extremely low, suggesting these elements can rapidly evaporate from the solid under high-temperature conditions.

recondense in situ. Nevertheless, δ^{66}Zn in PCA 02010 and B-7904 is notably heavy but not as extreme as in other samples, possibly because evaporation was partly restricted, allowing some vapor to be trapped or re-equilibrated. Alternatively, slightly higher local pressures (e.g., from abundant volatiles released at shallow burial depth) may have partially suppressed isotopic fractionation, resulting in more moderate δ^{66}Zn.

Impact-driven volatile depletion in asteroid parent bodies

The investigated carbonaceous chondrites provide the first unequivocal evidence of purely kinetic Zn isotope fractionation during volatilization from a solid state. By inducing sublimation, impacts facilitate evaporation in near-surface regions, even in the absence of melting, thereby driving extensive depletion of MVE such as Zn. Crucially, these collisions produce open-system conditions conducive to strong volatile escape. By comparison, internal heating processes (e.g., radioactive decay of ^{26}Al or ^{60}Fe) operate over much longer timescales (10^4–10^6 years) and tend to occur in more closed-system environments, enabling volatiles to be redistributed or sequestered internally. As impact-driven sublimation is effectively unconfined, the vapor rapidly escapes into space rather than recondensing locally. On a larger scale, the frequent high-energy impacts characteristic of the early Solar System would progressively strip volatiles from asteroidal surfaces (particularly given low gravity and an open escape path), eventually altering both the surface composition and deeper differentiation pathways. Notably, our findings reveal that even undifferentiated bodies likely show MVE depletion through purely kinetic, solid-state evaporation, emphasizing impacts as a key driver of volatile loss and heavy-isotope enrichment. Therefore, if volatile-poor, MVE-depleted chondritic material (resulting from collisional processing) contributed significantly to a growing planet's mass, the resulting bulk volatile budget might mask the expected signals from fully differentiated planetesimals. In other words, rather than MVE depletion being solely attributed to differentiation and core-mantle segregation processes, collisional history must also be considered as a fundamental mechanism that alters the initial volatile inventory.

Overall, collisional heating is capable of inducing extreme isotopic shifts and permanently depleting near-surface volatiles on parent bodies. Future models of planetary assembly should thus include the possibility that even undifferentiated chondritic precursors underwent substantial impact-driven volatilization, potentially imprinting the volatile inventories and isotopic compositions of terrestrial planets.

Methods

Major and trace elements

The elemental content of samples was analyzed using an Agilent 7900 Quadrupole Inductively Coupled Plasma Mass Spectrometry instrument at the Institut de Physique du Globe de Paris (IPGP), France. The sample was introduced into a Scott spray chamber through a MicroMist nebulizer at an uptake rate of 0.2 mL/min. Polyatomic interferences were mitigated by analyzing atomic masses from 23 (Na) to 75 (As) in a collision-reaction cell, utilizing helium gas at a flow rate of 5 mL/min. Internal standards, including Sc, In, and Re, were added to the sample solutions to correct for any signal drift and matrix effects. A mixture of certified standards was measured across a range of concentrations to convert count measurements into solution concentrations.

Zinc isotopes

Zinc isotopic measurements were conducted at IPGP using a Thermo Scientific Neptune Plus Multi-Collector Inductively-Coupled-Plasma Mass-Spectrometer. Approximately 35 mg of homogenized bulk powder from each sample (derived from a larger homogenized portion) was dissolved in a 1:3 mixture of concentrated HNO_3 (500 µL) and HF (1.5 mL) and heated at 120 °C for ~48 h. The acids were then evaporated, and the residues were processed with a 3:1 mixture of concentrated HCl (3 mL) and HNO_3 (1 mL) to dissolve any residual fluoride complexes. Samples were then evaporated to dryness and re-dissolved in 1.5 mol/L HBr (1 mL) for chemical purification. Procedures of sample pretreatment, chemical purification, and analytical methods are detailed in prior publications[17]. Isotope ratios were determined using the standard-sample-standard bracketing method with JMC-Lyon as the Zn isotope standard, expressed in the δ^xZn notation:

$$\delta^{x}\mathrm{Zn} = \left[\frac{\left(\frac{^{x}\mathrm{Zn}}{^{64}\mathrm{Zn}}\right)_{\mathrm{Sample}}}{\left(\frac{^{x}\mathrm{Zn}}{^{64}\mathrm{Zn}}\right)_{\mathrm{JMC-Lyon}}} - 1\right] \times 1000$$

where $X = 66$ and 68. The precision and reproducibility of chemical separation and isotopic analyses were monitored using terrestrial rock standard BHVO-2 and BCR-2, yielding δ^{66}Zn values of 0.29 ± 0.06‰ (2 SD, $n = 4$) and 0.25 ± 0.03‰ (2 SD, $n = 3$), respectively, aligning with published values[11]. The analytical results for Zn isotopes and bulk major and trace elements are detailed in Tables S1, S2.

Data availability

All data are available in the Supplementary Materials.

References

1. Scott, E. R. D. & Krot, A. N. *Chondrites and Their Components*. vol. 1 (Elsevier, 2014).
2. Alexander, C. M. O. D., Boss, A. P. & Carlson, R. W. The early evolution of the inner solar system: a meteoritic perspective. *Science* **293**, 64–68 (2001).
3. Galy, A., Young, E. D., Ash, R. D. & Keith O'Nions, R. The formation of chondrules at high gas pressures in the solar nebula. *Science* **290**, 1751–1753 (2000).
4. Alexander, C. M. O., Grossman, J. N., Ebel, D. S. & Ciesla, F. J. The formation conditions of chondrules and chondrites. *Science* **320**, 1617–1619 (2008).
5. Lodders, K. & Fegley, B. Jr. *Chemistry of the Solar System*. Vol. 476 (Royal Society and Chemistry Publication, 2010).
6. Palme, H., Lodders, K. & Jones, A. Solar system abundances of the elements. In: Andrew M. Davis (ed.) *Planets, Asteriods, Comets and The Solar System*2nd edn, Vol. 2, pp. 15–36 (Elsevier, 2014).
7. Braukmüller, N., Wombacher, F., Funk, C. & Münker, C. Earth's volatile element depletion pattern inherited from a carbonaceous chondrite-like source. *Nat. Geosci.* **12**, 564–568 (2019).
8. Yokoyama, T. et al. Samples returned from the asteroid Ryugu are similar to Ivuna-type carbonaceous meteorites. *Science* **379**, eabn7850 (2022).
9. Lauretta, D. S. et al. Asteroid (101955) Bennu in the laboratory: properties of the sample collected by OSIRIS-REx. *Meteorit. Planet. Sci.* **59**, 2453–2486 (2024).
10. Scott, E. R. D. Chondrites and the protoplanetary disk. *Annu. Rev. Earth Planet. Sci.* **35**, 577–620 (2007).
11. Moynier, F., Vance, D., Fujii, T. & Savage, P. The isotope geochemistry of zinc and copper. *Rev. Mineral. Geochem.* **82**, 543–600 (2017).
12. Luck, J.-M., Othman, D. B. & Albarède, F. Zn and Cu isotopic variations in chondrites and iron meteorites: early solar nebula reservoirs and parent-body processes. *Geochim. Cosmochim. Acta* **69**, 5351–5363 (2005).
13. Pringle, E. A., Moynier, F., Beck, P., Paniello, R. & Hezel, D. C. The origin of volatile element depletion in early solar system material: clues from Zn isotopes in chondrules. *Earth Planet. Sci. Lett.* **468**, 62–71 (2017).
14. Paquet, M. et al. Contribution of Ryugu-like material to Earth's volatile inventory by Cu and Zn isotopic analysis. *Nat. Astron.* **7**, 182–189 (2023).
15. Bishop, M. C. et al. The Cu isotopic composition of iron meteorites. *Meteorit. Planet. Sci.* **47**, 268–276 (2012).
16. Moynier, F., Blichert-Toft, J., Telouk, P., Luck, J.-M. & Albarède, F. Comparative stable isotope geochemistry of Ni, Cu, Zn, and Fe in chondrites and iron meteorites. *Geochim. Cosmochim. Acta* **71**, 4365–4379 (2007).
17. van Kooten, E. & Moynier, F. Zinc isotope analyses of singularly small samples (< 5 ng Zn): investigating chondrule-matrix complementarity in Leoville. *Geochim. Cosmochim. Acta* **261**, 248–268 (2019).
18. Albarède, F. Volatile accretion history of the terrestrial planets and dynamic implications. *Nature* **461**, 1227–1233 (2009).
19. Mahan, B., Moynier, F., Beck, P., Pringle, E. A. & Siebert, J. A history of violence: Insights into post-accretionary heating in carbonaceous chondrites from volatile element abundances, Zn isotopes and water contents. *Geochim. Cosmochim. Acta* **220**, 19–35 (2018).
20. Nakamura, T. Post-hydration thermal metamorphism of carbonaceous chondrites. *J. Mineral. Petrol. Sci.* **100**, 260–272 (2005).
21. Tonui, E. et al. Petrographic, chemical and spectroscopic evidence for thermal metamorphism in carbonaceous chondrites I: CI and CM chondrites. *Geochim. Cosmochim. Acta* **126**, 284–306 (2014).
22. Amsellem, E., Moynier, F., Mahan, B. & Beck, P. Timing of thermal metamorphism in CM chondrites: implications for Ryugu and Bennu future sample return. *Icarus* **339**, 113593 (2020).
23. Moynier, F. et al. Isotopic fractionation of zinc in tektites. *Earth Planet. Sci. Lett.* **277**, 482–489 (2009).
24. Herzog, G. F., Moynier, F., Albarède, F. & Berezhnoy, A. A. Isotopic and elemental abundances of copper and zinc in lunar samples, Zagami, Pele's hairs, and a terrestrial basalt. *Geochim. Cosmochim. Acta* **73**, 5884–5904 (2009).
25. Paniello, R. C., Day, J. M. D. & Moynier, F. Zinc isotopic evidence for the origin of the Moon. *Nature* **490**, 376–379 (2012).
26. Kato, C., Moynier, F., Valdes, M. C., Dhaliwal, J. K. & Day, J. M. D. Extensive volatile loss during formation and differentiation of the Moon. *Nat. Commun.* **6**, 7617 (2015).
27. Rodovská, Z. et al. Implications for behavior of volatile elements during impacts—zinc and copper systematics in sediments from the Ries impact structure and central European tektites. *Meteorit. Planet. Sci.* **52**, 2178–2192 (2017).
28. Day, J. M. D., Moynier, F., Meshik, A. P., Pradivtseva, O. V. & Petit, D. R. Evaporative fractionation of zinc during the first nuclear detonation. *Sci. Adv.* **3**, e1602668 (2017).
29. Day, J. M. D., van Kooten, E. M. M. E., Hofmann, B. A. & Moynier, F. Mare basalt meteorites, magnesian-suite rocks and KREEP reveal loss of zinc during and after lunar formation. *Earth Planet. Sci. Lett.* **531**, 115998 (2020).
30. Wimpenny, J. et al. Experimental determination of Zn isotope fractionation during evaporative loss at extreme temperatures. *Geochim. Cosmochim. Acta* **259**, 391–411 (2019).
31. Kamber, B. S. & Schoenberg, R. Evaporative loss of moderately volatile metals from the superheated 1849 Ma Sudbury impact melt sheet inferred from stable Zn isotopes. *Earth Planet. Sci. Lett.* **544**, 116356 (2020).
32. Mathur, R. et al. Fingerprinting the Cretaceous-Paleogene boundary impact with Zn isotopes. *Nat. Commun.* **12**, 4128 (2021).
33. Paquet, M., Sossi, P. A. & Moynier, F. Origin and abundances of volatiles on Mars from the zinc isotopic composition of Martian meteorites. *Earth Planet. Sci. Lett.* **611**, 118126 (2023).
34. Long, Z.-Y. et al. Constraining the evaporative loss of zinc during impact processes using terrestrial impact glasses. *Earth Planet. Sci. Lett.* **646**, 118979 (2024).
35. Day, J. M. D. & Moynier, F. Evaporative fractionation of volatile stable isotopes and their bearing on the origin of the Moon. *Philos. Trans. R. Soc. Math. Phys. Eng. Sci.* **372**, 20130259 (2014).
36. King, A. J. et al. The Yamato-type (CY) carbonaceous chondrite group: analogues for the surface of asteroid Ryugu? *Geochemistry* **79**, 125531 (2019).
37. Clayton, R. N. & Mayeda, T. K. Oxygen isotope studies of carbonaceous chondrites. *Geochim. Cosmochim. Acta* **63**, 2089–2104 (1999).
38. Zhu, K. et al. CY1 chondrites produced by impact-dehydration of the CI chondrite parent body. *Astrophys. J. Lett.* **984**, L54 (2025).
39. Schrader, D. L. et al. Reassessing the proposed "CY chondrites": evidence for multiple meteorite types and parent bodies from Cr-Ti-H-C-N isotopes and bulk elemental compositions. *Geochim. Cosmochim. Acta* **390**, 24–37 (2025).
40. Bell, M. S., Zolensky, M. E. & Yang, S. V. Evidence for thermal alteration in the Asuka 881655 chondrite. *Meteorit. Planet Sci.* **33**, A13 (1998).
41. Wang, M. & Lipschutz, M. E. Thermally metamorphosed carbonaceous chondrites from data for thermally mobile trace elements. *Meteorit. Planet. Sci.* **33**, 1297–1302 (1998).
42. Nakato, A. et al. PCA 02012: A unique thermally metamorphosed carbonaceous chondrite. *Lunar Planet Sci.* **44**, A2708 (2013).

43. Garenne, A. et al. The abundance and stability of "water" in type 1 and 2 carbonaceous chondrites (CI, CM and CR). *Geochim. Cosmochim. Acta* **137**, 93–112 (2014).
44. Alexander, C. M. O., Howard, K. T., Bowden, R. & Fogel, M. L. The classification of CM and CR chondrites using bulk H, C and N abundances and isotopic compositions. *Geochim. Cosmochim. Acta* **123**, 244–260 (2013).
45. Hu, Y., Moynier, F. & Yang, X. Volatile-depletion processing of the building blocks of Earth and Mars as recorded by potassium isotopes. *Earth Planet. Sci. Lett.* **620**, 118319 (2023).
46. Pringle, E. A. & Moynier, F. Rubidium isotopic composition of the Earth, meteorites, and the Moon: Evidence for the origin of volatile loss during planetary accretion. *Earth Planet. Sci. Lett.* **473**, 62–70 (2017).
47. Suttle, M. D. et al. The mineralogy and alteration history of the Yamato-type (CY) carbonaceous chondrites. *Geochim. Cosmochim. Acta* **361**, 245–264 (2023).
48. Naraoka, H. et al. A chemical sequence of macromolecular organic matter in the CM chondrites. *Meteorit. Planet. Sci.* **39**, 401–406 (2004).
49. Barrat, J. A. et al. Geochemistry of CI chondrites: Major and trace elements, and Cu and Zn isotopes. *Geochim. Cosmochim. Acta* **83**, 79–92 (2012).
50. Moynier, F. et al. Nature of volatile depletion and genetic relationships in enstatite chondrites and aubrites inferred from Zn isotopes. *Geochim. Cosmochim. Acta* **75**, 297–307 (2011).
51. Chen, H., Savage, P. S., Teng, F.-Z., Helz, R. T. & Moynier, F. Zinc isotope fractionation during magmatic differentiation and the isotopic composition of the bulk Earth. *Earth Planet. Sci. Lett.* **369–370**, 34–42 (2013).
52. King, A. J., Schofield, P. F. & Russell, S. S. Thermal alteration of CM carbonaceous chondrites: Mineralogical changes and metamorphic temperatures. *Geochim. Cosmochim. Acta* **298**, 167–190 (2021).
53. Hanna, R. D. et al. Distinguishing relative aqueous alteration and heating among CM chondrites with IR spectroscopy. *Icarus* **346**, 113760 (2020).
54. Suhr, N. et al. Elemental and isotopic behaviour of Zn in Deccan basalt weathering profiles: Chemical weathering from bedrock to laterite and links to Zn deficiency in tropical soils. *Sci. Total Environ.* **619–620**, 1451–1463 (2018).
55. Little, S. H. et al. Cu and Zn isotope fractionation during extreme chemical weathering. *Geochim. Cosmochim. Acta* **263**, 85–107 (2019).
56. Rubin, A. E., Trigo-Rodríguez, J. M., Huber, H. & Wasson, J. T. Progressive aqueous alteration of CM carbonaceous chondrites. *Geochim. Cosmochim. Acta* **71**, 2361–2382 (2007).
57. Young, E. D., Galy, A. & Nagahara, H. Kinetic and equilibrium mass-dependent isotope fractionation laws in nature and their geochemical and cosmochemical significance. *Geochim. Cosmochim. Acta* **66**, 1095–1104 (2002).
58. Young, E. D. & Galy, A. The Isotope Geochemistry and Cosmochemistry of Magnesium. *Rev. Mineral. Geochem.* **55**, 197–230 (2004).
59. Luck, J. M., Othman, D. B., Barrat, J. A. & Albarède, F. Coupled 63Cu and 16 O excesses in chondrites. *Geochim. Cosmochim. Acta* **67**, 143–151 (2003).
60. Fang, L. et al. The origin of 4-Vesta's volatile depletion revealed by the zinc isotopic composition of diogenites. *Sci. Adv.* **10**, eadl1007 (2024).
61. Bourdon, B. & Fitoussi, C. Isotope fractionation during condensation and evaporation during planet formation processes. *ACS Earth Space Chem.* **4**, 1408–1423 (2020).
62. Alexander, C. M. O. et al. The lack of potassium-isotopic fractionation in Bishunpur chondrules. *Meteorit. Planet. Sci.* **35**, 859–868 (2000).
63. Sossi, P. A. et al. An experimentally-determined general formalism for evaporation and isotope fractionation of Cu and Zn from silicate melts between 1300 and 1500 °C and 1 bar. *Geochim. Cosmochim. Acta* **288**, 316–340 (2020).
64. Jiang, Y. et al. Implications of K, Cu and Zn isotopes for the formation of tektites. *Geochim. Cosmochim. Acta* **259**, 170–187 (2019).
65. Langmuir, I. The evaporation, condensation and reflection of molecules and the mechanism of adsorption. *Phys. Rev.* **8**, 149–176 (1916).
66. Matza, S. D. & Lipschutz, M. E. Thermal metamorphism of primitive meteorites—VII. Mineralogy-petrology of heated Murchison (C2) and alteration of C30 and other chondrites. *Geochim. Cosmochim. Acta* **42**, 1655–1667 (1978).
67. Scott, E. R. D., Keil, K. & Stöffler, D. Shock metamorphism of carbonaceous chondrites. *Geochim. Cosmochim. Acta* **56**, 4281–4293 (1992).
68. Sossi, P. A. & Fegley, B. Thermodynamics of element volatility and its application to planetary processes. In: *High Temperature Gas-Solid Reactions in Earth and Planetary Processes* (eds. King, P., Fegley, B. & Seward, T.) 393–460. https://doi.org/10.1515/rmg.2018.84.11 (De Gruyter, 2018).
69. Creech, J. B. & Moynier, F. Tin and zinc stable isotope characterisation of chondrites and implications for early Solar System evolution. *Chem. Geol.* **511**, 81–90 (2019).
70. Sossi, P. A., Nebel, O., O'Neill, H. S.tC. & Moynier, F. Zinc isotope composition of the Earth and its behaviour during planetary accretion. *Chem. Geol.* **477**, 73–84 (2018).

Acknowledgements

K.F.Q. acknowledges financial support from the National Key R&D Program of China (grant 2023YFF0804200). F.M. acknowledges funding from the ERC under the European Community's H2020 framework program/ERC grant agreement No. 101001282 (METAL) and an International Emerging Action grant from the CNRS. Z.Y.L. acknowledges the financial support of the China Scholarship Council (202206400044). R.C. acknowledges financial support from Labex UnivEarthS and ICUB. J.D. acknowledges support from the NASA Solar System Workings Program (80NSSC22K0098). The calculations were performed thanks to the eDARI stl2816 grants. This study is also financially supported by the Frontiers Science Center for Deep-Time Digital Earth (grant 2652023001). We thank Samia Hidalgo for her assistance with the ICP-QMS analyses. We thank NASA and the National Institute for Polar Research, Japan, for the meteorites. Parts of this work were supported by IPGP multidisciplinary program PARI, by Region Île-de-France SESAME Grants no. 12015908, EX047016, and the IdEx Université de Paris grant, ANR–18-IDEX-0001 and the DIM ACAV+.

Author contributions

Z.Y.L. and F.M. designed the project. Z.Y.L., L.F., T.H.L. and D.R. conducted the experiments and chemical analyses. T.F.J.B. and R.C. conducted the first-principles calculations. M.P., F.J., K.F.Q., J.D. and J.M.D.D. contributed to the interpretation and discussion of the results. All authors participated in writing, reviewing, and editing the manuscript.

Competing interests

The authors declare no competing interests.

Additional information

Supplementary information The online version contains supplementary material available at https://doi.org/10.1038/s41467-025-61115-3.

Correspondence and requests for materials should be addressed to Zheng-Yu Long or Frederic Moynier.

Peer review information *Nature Communications* thanks Philippe Claeys and the other, anonymous, reviewer for their contribution to the peer review of this work. A peer review file is available.